

Fusion reaction studies for the ${}^6\text{Li} + {}^{90}\text{Zr}$ system at near-barrier energiesH. Kumawat,^{1,*} V. Jha,¹ V. V. Parkar,^{1,2} B. J. Roy,¹ S. K. Pandit,¹ R. Palit,² P. K. Rath,³ C. S. Palshetkar,¹ Sushil K. Sharma,² Shital Thakur,² A. K. Mohanty,¹ A. Chatterjee,¹ and S. Kailas¹¹*Nuclear Physics Division, Bhabha Atomic Research Centre, Mumbai 400085, India*²*Department of Nuclear and Atomic Physics, Tata Institute of Fundamental Research, Mumbai 400005, India*³*Department of Physics, Maharaja Sayajirao University of Baroda, Vadodra 390002, India*

(Received 20 June 2012; published 24 August 2012)

Complete fusion cross sections have been measured using the off-line γ -ray spectroscopy method for the ${}^6\text{Li} + {}^{90}\text{Zr}$ system around barrier energies. Statistical and coupled-channel calculations have been performed to investigate the effect of coupling on complete fusion. It is observed that the complete fusion is suppressed by $34 \pm 8\%$ compared to the coupled channel predictions. The effect of breakup coupling is estimated using the continuum discretized coupled channels (CDCC) method and it is found to reduce the complete fusion probability. Contrary to earlier predictions, a universal behavior of complete fusion suppression factor for the ${}^6\text{Li}$ projectile with target charge is observed.

DOI: [10.1103/PhysRevC.86.024607](https://doi.org/10.1103/PhysRevC.86.024607)

PACS number(s): 25.70.Jj, 25.70.Gh, 25.70.Mn

I. INTRODUCTION

Fusion of two colliding nuclei around the Coulomb barrier is a complex phenomena. Quantum mechanical barrier penetration occurs in a multidimensional space and coupling to the internal degrees of freedom of the participating nuclei plays an important role. There are several interesting features associated with the fusion process. Experimentally measured sub-barrier fusion cross sections for tightly bound nuclei are enhanced [1–4] by several orders of magnitude over the predictions of the simple one-dimensional barrier penetration models (1DBPM). The observed enhancement is understood in terms of couplings to the low-lying collective excited states of target and projectile and to transfer of one or more nucleons. Understanding the fusion process with weakly bound nuclei, either stable or short-lived, brings in a new set of challenges. To start with, the definition of fusion cross section itself needs to be clarified. There are similar processes such as the incomplete fusion (ICF), wherein only part of the projectile fuses with the target. Hence, a distinction needs to be made wherever possible between complete fusion (CF), which involves the fusion of the projectile as a whole with the target, and total fusion (TF), which also includes the ICF component.

In general, the reaction cross section for weakly bound nuclei is found to be much larger as compared to that for the corresponding tightly bound nuclei [5]. But unlike the tightly bound nuclei where the fusion cross section accounts for the major part of the reaction cross section at near-barrier energies, the contribution of direct reaction channels, such as breakup and transfer is significant in case of the weakly bound nuclei [6]. The complete fusion cross sections for weakly bound nuclei at energies above the Coulomb barrier show a large suppression as compared to predictions of 1DBPM. However, there have been conflicting experimental results and theoretical interpretations [7–10] regarding suppression or enhancement of fusion cross sections as compared with coupled-channel

calculations. The detailed treatment of breakup using the continuum discretized coupled channels (CDCC) approach shows that the continuum-continuum couplings lead to fusion suppression at all energies [11,12]. In spite of extensive work [13–18], there is not a definitive explanation of the influence of breakup and transfer on fusion for the weakly bound systems.

A consistent correlation of complete fusion suppression factor with breakup threshold energy of the ${}^6,7\text{Li}$, ${}^9\text{Be}$, and ${}^{10,11}\text{B}$ projectiles [19] was found with heavy targets. Generally, experimental data seem to indicate that the magnitude of CF suppression above the barrier may be consistent with the yield of incomplete fusion [20]. The behavior of the suppression for different targets deduced from coupled-channel calculations are contradictory [13,19,21]. Based on the ICF measurement for ${}^9\text{Be}$ on heavy targets, it was predicted [20,21] that the complete fusion suppression factor will decrease with target charge. Even for the ${}^6\text{Li}$ projectile, the CF suppression factor was expected [13] to decrease with target charge. Therefore, fusion measurements are necessary for light mass systems to study the systematic behavior of the CF suppression factor. The breakup due to Coulomb and nuclear processes are expected to contribute to the CF and the ICF in a different way.

The disentangling of CF and ICF becomes difficult for the light mass systems where these components are mixed up. Therefore, it is important to perform experimental measurements for the systems where CF and ICF cross sections can be measured separately. In this context, we report the measurement of the CF cross sections for the ${}^6\text{Li} + {}^{90}\text{Zr}$ system at near-barrier energies. Due to the low breakup threshold of ${}^6\text{Li}$, the dominant contribution from the couplings to the breakup channel is expected. A very significant breakup threshold anomaly was found [22] to exist for this system, which has been explained in terms of the breakup coupling due to the nuclear part of the potential. Further, the analysis of the α -production cross section in Ref. [23] shows that the $1n$ transfer contribution is more than the exclusive breakup cross section over the whole energy range.

The article is organized as follows. In Sec. II we present experimental details regarding the measurements. Section III

* Corresponding author: harphool@barc.gov.in

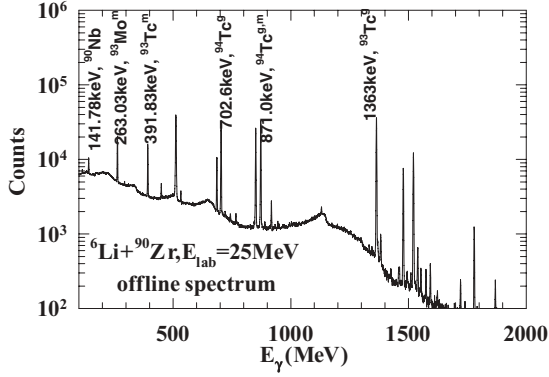


FIG. 1. The off-line γ -ray spectrum depicting the γ lines of evaporation residues (ERs) populated for the ${}^6\text{Li} + {}^{90}\text{Zr}$ system at the projectile energy of 25 MeV.

contains the analysis procedure to obtain the experimental results. Section IV describes the coupled-channel calculations. Breakup coupling effects are presented in Sec. V. The systematic behavior of CF suppression is discussed in Sec. VI and a summary is presented in Sec. VII.

II. EXPERIMENT DETAILS

The experiment was performed using a ${}^6\text{Li}^{3+}$ beam delivered by the 14UD Pelletron accelerator of Bhabha Atomic Research Centre/Tata Institute of Fundamental Research (TIFR/BARC) Facility in Mumbai, India at bombarding energies from 13–30 MeV. The beam energies were corrected for the half target thickness in the analysis process and the correction was a minimum of 88 keV for 30 MeV and a maximum of 132 keV for 13 MeV. Beam current was typically in the range of 5–30 pA. The beam impinged on a $\sim 500 \mu\text{g}/\text{cm}^2$, self-supported enriched ${}^{90}\text{Zr}$ (>99%) target. The irradiation was done using several targets of thickness $\sim 500 \mu\text{g}/\text{cm}^2$. In all the irradiations, aluminum catcher foils of thickness $\sim 1 \text{ mg}/\text{cm}^2$ were used along with the target to stop the recoiling ERs. Each irradiation was done for 4–6 hours and counting was started after ~ 5 minutes. Beam current was recorded using a CAMAC scalar in a list mode. One high-purity germanium (HPGe) detector of resolution $\sim 2 \text{ keV}$ at 1332 keV γ line of ${}^{60}\text{Co}$ source was used to measure the decay γ lines. The absolute efficiency and energy calibration of the detector were achieved using a set of standard radioactive sources (${}^{152}\text{Eu}$, ${}^{133}\text{Ba}$, and ${}^{60}\text{Co}$) mounted in the same geometry as the target. The typical spectrum for the off-line measurement is given in Fig. 1. Several identified channels from radioactive decay are denoted in the spectra.

III. ANALYSIS OF EXPERIMENTAL RESULTS

The compound nucleus formed by the complete fusion of the ${}^6\text{Li} + {}^{90}\text{Zr}$ system is ${}^{96}\text{Tc}$. A list of ERs populated through various channels due to evaporation of ${}^{96}\text{Tc}$, their half-lives, prominent γ -line energy of decay, and intensity of the γ lines, are given in Table I.

TABLE I. The physical properties of the populated evaporation residues either by CF, ICF or transfer (TR) reactions. Some of the dominant γ lines from decay of ERs along with intensities are given.

Reactions	ER	J^π	$T_{1/2}$	E_γ	$I_\gamma(\%)$
${}^{90}\text{Zr}({}^6\text{Li}, 1n)$	${}^{95}\text{Tc}^g$	$9/2^+$	20 h	765.8	93.82
${}^{90}\text{Zr}({}^6\text{Li}, 1n)$	${}^{95}\text{Tc}^m$	$1/2^-$	61 d	38.9	100
${}^{90}\text{Zr}({}^6\text{Li}, 2n)$	${}^{94}\text{Tc}^g$	7^+	293 m	702.6	99.6
${}^{90}\text{Zr}({}^6\text{Li}, 2n)$	${}^{94}\text{Tc}^m$	2^+	52 m	871	94.1
${}^{90}\text{Zr}({}^6\text{Li}, 3n)$	${}^{93}\text{Tc}^g$	$9/2^+$	2.75 h	1363	66
${}^{90}\text{Zr}({}^6\text{Li}, 3n)$	${}^{93}\text{Tc}^m$	$1/2^-$	43.5 m	391.8	58
${}^{90}\text{Zr}({}^6\text{Li}, 1p2n)$	${}^{93}\text{Mo}^m$	$21/2^+$	6.85 h	263.08	56.7
${}^{90}\text{Zr}({}^6\text{Li}, X)$	${}^{90}\text{Nb}^g$	8^+	14.60 h	1129.2	92.7

The experimental ER cross section for the off-line measurement is obtained using Eq. (1),

$$\sigma_{\text{ER}}^{\text{expt}} = \frac{Y\lambda}{N_t \epsilon I_\gamma X}, \quad (1)$$

where

$$X = \sum_{n=1}^m I_n (1 - e^{-\lambda t_{\text{step}}}) e^{-\lambda(n-1)t_{\text{step}}} (e^{-\lambda t_1} - e^{-\lambda t_2}), \quad (2)$$

Y is the yield of the γ line, λ is the disintegration constant of the ER, N_t is the target atoms/cm², ϵ is the efficiency of the detector for the γ line, I_γ is the absolute intensity of the γ line in time t_{step} , $t_2 - t_1$ is the measurement time, and t_{step} is the time step in which the beam current was recorded. The sum is over all the recorded beam times. The ERs [${}^{94}\text{Tc}$ ($2n$ channel), ${}^{93}\text{Tc}$ ($3n$ channel), ${}^{93}\text{Mo}^m$ ($1p2n$ channel), and ${}^{90}\text{Nb}$] are identified using the γ line along with the half lives.

The measured cross sections for $2n$ and $3n$ channels are compared with the statistical model predictions using CASCADE [24]. The calculated and experimental ratio of $3n$ to $2n$ channel is plotted in Fig. 2, which agrees well with the experimental ratio. The $3n + 2n$ contributes 59–84% of the complete fusion cross sections. The other ERs, such as ${}^{93}\text{Mo}$ and ${}^{90}\text{Nb}$ are populated with the mixture of metastable and ground state, and we could measure only ${}^{93}\text{Mo}^m$ and ${}^{90}\text{Nb}^g$. It is to be mentioned that ${}^{93}\text{Mo}$ can also be populated by the α transfer or incomplete fusion followed by neutron evaporation. Both ERs (${}^{93}\text{Mo}^m$ and ${}^{90}\text{Nb}^g$) are observed only at 25- and 30-MeV energies. Due to these reasons, we have not considered these ERs for deducing the fusion cross sections. The remaining CF part is estimated with the help of statistical model code. The ratio $R = \sum_x \sigma_{xn}^{\text{CASCADE}} / \sigma_{\text{fus}}^{\text{CASCADE}}$ is calculated and CF is obtained by $\sigma_{\text{fus}}^{\text{expt}} = \sum_x \sigma_{xn}^{\text{expt}} / R$. The ratio is not sensitive to the level density parameter ($A/8$, $A/9$, $A/10$) even though the absolute values are different for these values. The statistical model calculations for $2n$ and $3n$ channels are again performed using the experimental fusion data (estimated above) as input to the CASCADE. The experimental cross sections for $2n$ and $3n$ channels are plotted in Fig. 2 and it agrees well with the values obtained from the CASCADE (denoted as CASCADE, fusion input). The CF cross sections are given in Table II. The errors in the table are the sum of statistical error and errors due to fitting ($\sim 2\%$), target thickness ($\sim 2\%$), efficiency ($\sim 3\%$), and the error due to the

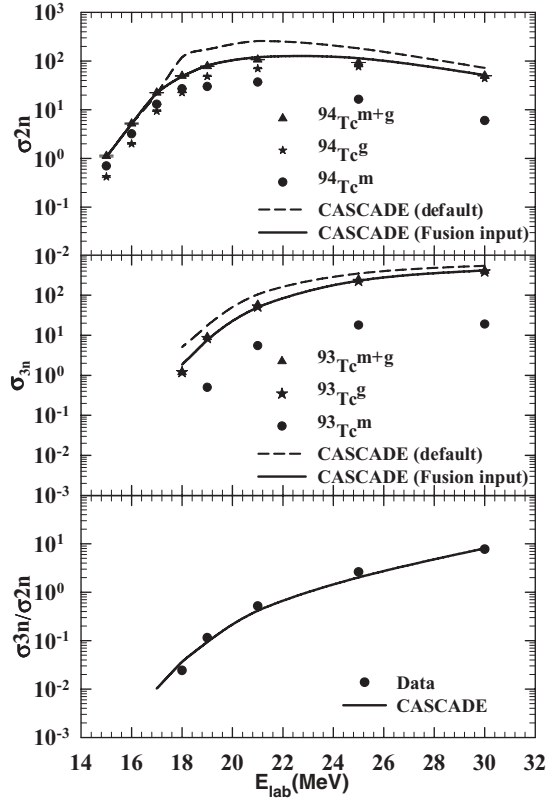


FIG. 2. Evaporation residue cross sections for ground state (star), metastable state (circle), and total (m + g, triangle), CASCADE with default parameters (dashed line) and CASCADE with experimental fusion cross section input (solid line) of (a) ${}^{94}\text{Tc}$, $2n$ channel, (b) ${}^{93}\text{Tc}$, $3n$ channel, (c) measured and CASCADE predicted ratio of σ_{3n} to σ_{2n} at different projectile energies.

maximum likelihood fit when 2–3 γ lines were used to get the cross section of the ERs. The direct population to the ground state of the ERs are expected to be small in this mass region [25] but it could not be estimated in the present off-line analysis technique.

IV. COUPLED-CHANNEL CALCULATIONS

Coupled-channel (CC) calculations are performed using the modified version of CCFULL [26], which allows the coupling

TABLE II. Experimental complete fusion cross sections and the ratio R (as defined in the text) for the ${}^6\text{Li} + {}^{90}\text{Zr}$ system at the measured energies.

E_{lab} (MeV)	$E_{\text{c.m.}}$ (MeV)	R	σ_{CF} (mb)
29.9	28.0	0.59	778 ± 37
24.9	23.3	0.66	510 ± 24
20.9	19.6	0.72	230 ± 11
18.9	17.7	0.76	114 ± 7
17.9	16.8	0.80	63 ± 4
16.9	15.8	0.82	27 ± 2
15.9	14.9	0.83	6.3 ± 0.6
14.9	13.9	0.84	1.3 ± 0.2

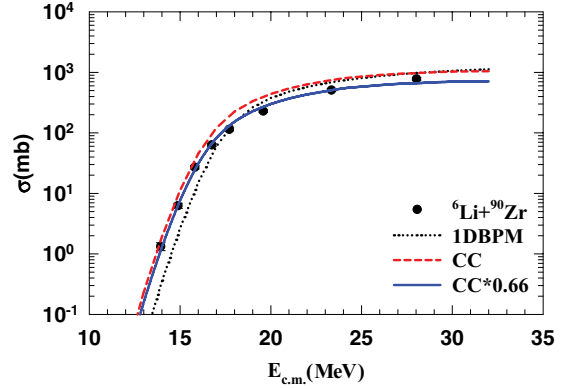


FIG. 3. (Color online) CF (circles) cross section for the ${}^6\text{Li} + {}^{90}\text{Zr}$ system. Theoretical analysis using 1DBPM, Coupled channel (CC), and CC*0.66 are shown by dotted line, dashed line, and full line, respectively.

of projectile excited states and it includes the effect of the projectile spin. The initial input potential parameters for CCFULL are obtained from the Woods-Saxon parametrization of the Akyuz-Winther (AW) potential ($V_0 = 43.35$ MeV, $r_0 = 1.17$ fm, $a = 0.606$). The potential is slightly modified to fit the fusion barrier distribution ($V_0 = 47.5$ MeV, $r_0 = 1.11$ fm, $a = 0.66$). The derived values for the uncoupled barrier heights are $V_B = 17.2$ MeV, radius $R_B = 9.32$ fm, and the curvature is $\hbar\omega = 4.22$ MeV. The projectile ground state (1^+) with the quadrupole moment, $Q = -0.082$ fm 2 , and the unbound first excited state (3^+ , 2.186 MeV) are coupled. A value of $B(E2; 1^+ \rightarrow 3^+) = 21.8$ e 2 fm 4 is used for the 3^+ rotational excitation (same as in Ref. [27]). The target excited states (3^- , 2.747 MeV or 2^+ , 2.186 MeV) are coupled as the vibrational states. Coupling of the nonresonant breakup channel is not considered in these calculations.

The results of the coupled-channel calculations are shown in Fig. 3. It can be seen from Fig. 3 that at energies below the Coulomb barrier, the coupled calculations (dashed line) show an enhancement of fusion cross section as compared to the uncoupled ones (dotted lines). But the coupled results overestimate the measured fusion data for all energies. However, the measured fusion cross sections agree very well with the calculated ones when multiplied by an overall factor of 0.66 (solid line). The mean suppression factor (F_{CF}) is deduced from a least square fit to the suppression factors obtained over the entire energy range (see Fig. 4). This implies that there is an overall suppression of the complete fusion cross section by $\sim 34\%$ as compared to the ones predicted by CCFULL. An uncertainty up to $\sim 8\%$ in the suppression factor is estimated due to the errors in the measured fusion cross sections.

V. BREAKUP COUPLING EFFECT

Detailed studies of coupling effects due to the projectile breakup on the fusion have been performed using the CDCC framework. We have used the code FRESKO to perform the calculations. Two approaches have been followed to determine the fusion cross sections. In the first method, the fusion is calculated according to the barrier penetration

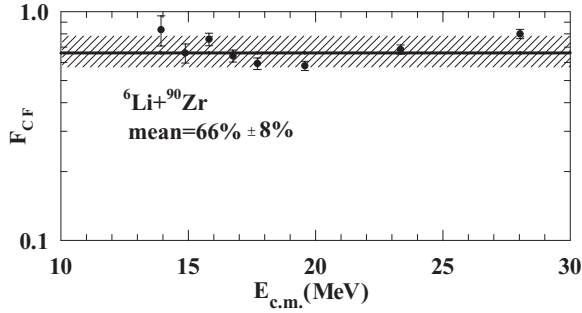


FIG. 4. Suppression factor (F_{CF}) at each energy and the least square fit to the data to obtain the mean value and error for the ${}^6\text{Li} + {}^{90}\text{Zr}$ system.

model using an effective potential, which consists of the bare cluster-folded potential and the equivalent polarization potential generated from the couplings. In the second method, the cumulative absorption cross section by the long-range imaginary potential is calculated, which equals the sum of the total fusion (CF + ICF), transfer and inelastic cross sections. The complete fusion cross section could in principle be derived by subtracting the other components.

In the calculations, the ${}^6\text{Li}$ nucleus is assumed to have a two-body $\alpha + d$ cluster structure with the breakup threshold equal to 1.473 MeV. The CDCC calculations require the $\alpha + {}^{90}\text{Zr}$ and the $d + {}^{90}\text{Zr}$ optical potentials as an input to generate the ${}^6\text{Li} + {}^{90}\text{Zr}$ optical potential by the single-folding technique. These potentials are obtained from the global potential for α [28] and d [29] optical model potentials. The real part of the global potential strength for the $\alpha + {}^{90}\text{Zr}$ system was renormalized by a factor of 0.45 in order to fit the elastic scattering data for the ${}^6\text{Li} + {}^{90}\text{Zr}$ system [22]. The potential used for $d + {}^{90}\text{Zr}$ is the unmodified potential from Ref. [29]. The details of the continuum discretization are the same as described in Ref. [23].

The fusion cross sections obtained by the barrier penetration model and the cumulative absorption from the CDCC calculations are shown in Fig. 5. The BPM fusion cross sections calculated with only the bare cluster-folded potential and

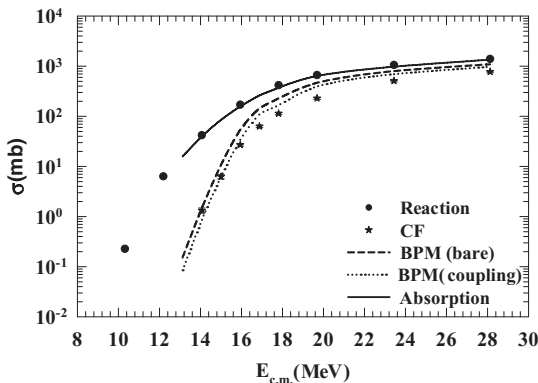


FIG. 5. Reaction (circles), CF (stars) cross section for the ${}^6\text{Li} + {}^{90}\text{Zr}$ system. The cross section predicted using the CDCC 1DBPM, BPM + breakup coupling, and the absorption model are shown by dashed, dotted, and solid lines, respectively.

with a potential that also includes the equivalent polarization potential generated from the breakup couplings are represented by dotted and dashed lines, respectively. The calculated absorption cross sections with the breakup couplings (denoted by solid line in Fig. 5) are close to the reaction cross sections, since the measured exclusive breakup cross section [30–32] is only 5–10% of the total reaction cross section. The calculated fusion cross sections with breakup coupling are systematically lower than the uncoupled cross sections at energies above the Coulomb barrier. As described in Ref. [23], the dynamic polarization potential generated due to the breakup coupling using the CDCC calculations are found to be repulsive around the nuclear surface region for all the beam energies. Therefore, the effective barrier is raised and there is a reduction in the penetration of the flux from the entrance channel leading to less fusion cross sections calculated from the 1DBPM over all energy range. Thus, the CDCC results, which take into account the projectile breakup are qualitatively consistent with the observed fusion suppression.

VI. DISCUSSION

The suppression factor of the measured complete fusion cross section for the ${}^6\text{Li} + {}^{90}\text{Zr}$ system is deduced. The mean suppression factor of $\sim 66\%$ is obtained in the measured energy range as compared to the coupled-channel calculations using CCFULL. The complete fusion suppression factor F_{CF} for ${}^6\text{Li}$ projectile with different targets is plotted in Fig. 6. The suppression factor for above barrier energies follows the systematic trend of breakup threshold dependence, which was also shown by Gasques *et al.* [19].

In order to study dependence of the complete fusion suppression factor on target charge, CC calculations for ${}^6\text{Li} + {}^{59}\text{Co}$ and ${}^6\text{Li} + {}^{28}\text{Si}$ systems have also been performed. To deduce the CF for these systems, it is assumed that the sum

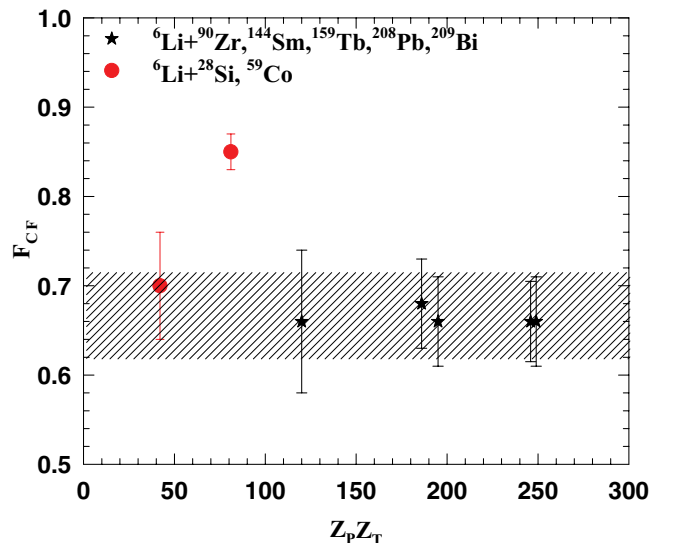


FIG. 6. (Color online) Universal complete fusion suppression factor (F_{CF}) for ${}^6\text{Li}$ projectile with different targets. The experimental data are taken from Refs. [8,13,33–35]

of direct inclusive- α and complete fusion cross sections equals the reaction cross section. This assumption is reasonably supported by many previous measurements [23,36,37], where the reaction and the α -production cross sections are measured. However, the separation of compound and direct contribution to the α -production cross sections is crucial here. The reaction and direct α -production cross sections for the ${}^{59}\text{Co}$ are taken from Ref. [33] and the CC coupling parameters are same as those given in Ref. [27]. It is shown that the complete fusion cross sections are suppressed by $\sim 15\%$ as compared to the values predicted by CCFULL. The odd behavior of this system might be due to underestimation of direct α -production cross sections. The experimental reaction and deduced direct α -production cross sections for ${}^{28}\text{Si}$ are taken from Ref. [38]. The CC coupling parameters are same as given in Ref. [39]. The complete fusion is suppressed by $\sim 30\%$ as compared to the values predicted by CCFULL.

It is observed that the suppression factor is independent of the charge of target nucleus except for the case of ${}^{59}\text{Co}$. The conclusion drawn in Ref. [13], that the complete fusion suppression factor decreases with the charge of the target, is not observed. The observation of a constant F_{CF} is consistent with the universal [23] behavior of the total inclusive α -production cross section observed for the ${}^6\text{Li}$ projectile with all the targets. Further, in our earlier work, we have shown [22] that the dynamic polarization potential arising due to the breakup of the ${}^6\text{Li}$ projectile is dominated by the nuclear breakup effect for all target systems and the role of Coulomb breakup is not significant. The dominance of nuclear over Coulomb coupling in the polarization potential was also found for the ${}^6\text{Li} + {}^{208}\text{Pb}$ system [40]. Therefore, it can be deduced that

the ICF component, which is supposed to supplement the loss of flux from the total fusion, may not decrease with the target charge as has been proposed in earlier studies. Further measurements in the lower mass region in which CF and ICF can be separated, are required to confirm the universal behavior of the complete fusion suppression.

VII. SUMMARY

The complete fusion excitation function for the ${}^6\text{Li} + {}^{90}\text{Zr}$ around the barrier energies are measured using the γ -ray spectroscopy technique. The cross sections measured for $2n$ and $3n$ evaporation channels along with the statistical model calculations are used to deduce the complete fusion cross sections. The complete fusion cross sections are observed to be suppressed by $34 \pm 8\%$ at all energies as compared to the coupled-channel predictions using CCFULL. The complete fusion suppression factor is observed to exhibit a universal behavior, irrespective of the target charge for the ${}^6\text{Li}$ projectile.

ACKNOWLEDGMENTS

The authors thank the Bhabha Atomic Research Centre/Tata Institute of Fundamental Research (BARC/TIFR) Pelletron staff for excellent delivery of the beam. We would like to thank to Dr. V. Nanal, Dr. S. Kumar, A. Shrivastava, and K. Mahata for their help during the experiment. V.V.P. acknowledges the support of a DST-INSPIRE grant from the Government of India in carrying out these investigations. Authors are grateful to the Research Centre, Jülich for providing us with an enriched ${}^{90}\text{Zr}$ target.

-
- [1] M. Dasgupta, D. J. Hinde, N. Rowley, and A. M. Stefanini, *Annu. Rev. Nucl. Part. Sci.* **48**, 401 (1998).
- [2] S. G. Steadman and M. J. Rhoades-Brown, *Annu. Rev. Nucl. Part. Sci.* **36**, 649 (1986).
- [3] J. D. Bierman, P. Chan, J. F. Liang, M. P. Kelly, A. A. Sonzogni, and R. Vandenbosch, *Phys. Rev. Lett.* **76**, 1587 (1996).
- [4] A. M. Stefanini *et al.*, *Phys. Rev. Lett.* **74**, 864 (1995).
- [5] E. F. Aguilera *et al.*, *Phys. Rev. Lett.* **107**, 092701 (2011).
- [6] E. A. Benjamim *et al.*, *Phys. Lett. B* **647**, 30 (2007).
- [7] V. Tripathi, A. Navin, K. Mahata, K. Ramachandran, A. Chatterjee, and S. Kailas, *Phys. Rev. Lett.* **88**, 172701 (2002).
- [8] M. Dasgupta *et al.*, *Phys. Rev. C* **70**, 024606 (2004).
- [9] J. Takahashi *et al.*, *Phys. Rev. Lett.* **78**, 30 (1997).
- [10] A. Mukherjee *et al.*, *Phys. Lett. B* **636**, 91 (2006).
- [11] A. Diaz-Torres and I. J. Thompson, *Phys. Rev. C* **65**, 024606 (2002).
- [12] V. Jha and S. Kailas, *Phys. Rev. C* **80**, 034607 (2009).
- [13] P. K. Rath *et al.*, *Phys. Rev. C* **79**, 051601(R) (2009).
- [14] V. V. Parkar *et al.*, *Phys. Rev. C* **82**, 054601 (2010).
- [15] L. F. Canto, P. R. S. Gomes, R. Donangelo, and M. S. Hussein, *Phys. Rep.* **424**, 1 (2006).
- [16] K. Rusek, N. Alamanos, N. Keeley, V. Lapoux, and A. Pakou, *Phys. Rev. C* **70**, 014603 (2004).
- [17] K. Rusek, *Eur. Phys. J. A* **41**, 399 (2009).
- [18] S. Kailas, V. Jha, H. Kumawat, and V. V. Parkar, *Nucl. Phys. A* **834**, 155c (2010).
- [19] L. R. Gasques, D. J. Hinde, M. Dasgupta, A. Mukherjee, and R. G. Thomas, *Phys. Rev. C* **79**, 034605 (2009).
- [20] D. J. Hinde, M. Dasgupta, B. R. Fulton, C. R. Morton, R. J. Wooliscroft, A. C. Berriman, and K. Hagino, *Phys. Rev. Lett.* **89**, 272701 (2002).
- [21] P. R. S. Gomes, R. Linares, J. Lubian, C. C. Lopes, E. N. Cardozo, B. H. F. Pereira, and I. Padron, *Phys. Rev. C* **84**, 014615 (2011).
- [22] H. Kumawat *et al.*, *Phys. Rev. C* **78**, 044617 (2008).
- [23] H. Kumawat *et al.*, *Phys. Rev. C* **81**, 054601 (2010).
- [24] F. Fuhlhofer, *Nucl. Phys. A* **280**, 267 (1977).
- [25] S. Cavallaro, L. Y. Xiao, M. L. Sperduto, and J. Delaunay, *Nucl. Instrum. Methods Phys. Res., Sect. A* **245**, 89 (1986).
- [26] K. Hagino, N. Rowley, and A. T. Kruppa, *Comput. Phys. Commun.* **123**, 143 (1999).
- [27] C. Beck *et al.*, *Phys. Rev. C* **67**, 054602 (2003).
- [28] A. Kumar *et al.*, *Nucl. Phys. A* **776**, 105 (2006).
- [29] C. M. Perey and F. G. Perey, *Phys. Rev.* **132**, 755 (1963).
- [30] A. Pakou *et al.*, *Phys. Lett. B* **633**, 691 (2006).
- [31] C. Signorini *et al.*, *Phys. Rev. C* **67**, 044607 (2003).
- [32] A. Shrivastava *et al.*, *Phys. Lett. B* **633**, 463 (2006).
- [33] F. A. Souza *et al.*, *Nucl. Phys. A* **821**, 36 (2009).
- [34] Y. W. Wu, Z. H. Liu, C. J. Lin, H. Q. Zhang, M. Ruan, F. Yang, Z. C. Li, M. Trotta, and K. Hagino, *Phys. Rev. C* **68**, 044605 (2003).

- [35] M. K. Pradhan *et al.*, [Phys. Rev. C **83**, 064606 \(2011\)](#).
- [36] S. Santra, S. Kailas, V. V. Parkar, K. Ramachandran, V. Jha, A. Chatterjee, P. K. Rath, and A. Parihari, [Phys. Rev. C **85**, 014612 \(2012\)](#).
- [37] C. Signorini *et al.*, [Eur. Phys. J. A **10**, 249 \(2001\)](#).
- [38] A. Pakou *et al.*, [J. Phys. G: Nucl. Part. Phys. **31**, S1723 \(2005\)](#).
- [39] M. Sinha *et al.*, [Eur. Phys. J. A **44**, 403 \(2010\)](#).
- [40] N. Keeley and K. Rusek, [Phys. Lett. B **427**, 1 \(1998\)](#).